Article

Co-culture model of Caco-2/HT29-MTX cells: a promising tool for investigation of phycotoxins toxicity on the intestinal barrier

Océane Reale, Antoine Huguet and Valérie Fessard*

ANSES, Fougères Laboratory, Toxicology of Contaminants Unit, French Agency for Food, Environmental and Occupational Health & Safety, Fougères 35306, France; oceane.reale@anses.fr; antoine.huguet@anses.fr; valerie.fessard@anses.fr

* Correspondence: valerie.fessard@anses.fr

Abstract:

Most lipophilic phycotoxins have been involved in human intoxications but some of these toxins have never been proven to induce human gastro-intestinal symptoms, although intestinal damage in rodents has been documented. For investigating the *in vitro* toxicological profile of lipophilic phycotoxins on intestine, the epithelial Caco-2 cell line has been the most commonly used model. Nevertheless, considering the complexity of the intestinal epithelium, *in vitro* co-cultures integrating enterocyte-like and mucus-secreting cell types are expected to provide more relevant data. In this study, the toxic effects (viability, inflammation, cellular monolayer integrity, modulation of cell type proportion and production of mucus) of four lipophilic phycotoxins (PTX2, YTX, AZA1 and OA) were evaluated in Caco-2/HT29-MTX co-cultured cells. The four toxins induced a reduction of viability from 20% to 50% and affected the monolayer integrity. Our results showed that the HT29-MTX cells population were more sensitive to OA and PTX2 than Caco-2 cells. Among the four phycotoxins, OA induced inflammation (28-fold increase of IL-8 release) and also a slight increase of both mucus production (up-regulation of mucins mRNA expression) and mucus secretion (mucus area and density). For PTX2 we observed an increase of IL-8 release but weaker than OA. Intestinal cell models integrating several cell types can contribute to improve hazard characterization and to describe more accurately the modes of action of phycotoxins.

Keywords: co-culture, Caco-2, HT29-MTX, phycotoxin, toxicity, intestine

1. Introduction

Phycotoxins, natural metabolites produced by unicellular micro-algae, can accumulate along the marine food web, especially in filter-feeding bivalves (Reguera et al., 2014). The consumption of contaminated seafood can provoke intoxications in humans depicted by various symptoms (Valdiglesias et al., 2013; Khora and Jal, 2018). Among the lipophilic phycotoxins, azaspiracid-1 (AZA1) and okadaic acid (OA) are known to induce general weakness, nausea, diarrhea, abdominal pains and vomiting (Twiner et al., 2008; Valdiglesias et al., 2013; Vilarino et al., 2018). In contrast, no human intoxications have been proven with pectenotoxin 2 (PTX2) and yessotoxin (YTX) (EFSA,

2008, 2009; Dominguez et al., 2010), despite acute toxic effects described in rodents (Ishige et al., 1988; Ogino et al., 1997; Aune et al., 2002; Callegari et al., 2006; Ito, 2006; Aasen et al., 2011).

The gastrointestinal epithelium acts as a barrier limiting the crossing of hazardous substances such as phycotoxins, and consequently the potential toxicity to systemic organs. Nevertheless, phycotoxins have been shown to induce some local toxicity in mice with macroscopical intestinal damage such as cell detachment, fluid accumulation, villous erosion and dilatation of intestine tract (Ishige et al., 1988; Ito et al., 2000; Ito et al., 2002; Ito et al., 2008; Aasen et al., 2010; Aune et al., 2012). Besides, infiltration of immune cells in the lamina propria was reported in previous studies (Terao et al., 1986; Aasen et al., 2011; Aune et al., 2012; Sosa et al., 2013; Kilcoyne et al., 2014).

If animal experiments remain crucial for addressing hazard characterization, design of *in vivo* studies with phycotoxins is hampered due to the cost and the low availability of these substances. Therefore, the use of human *in vitro* cell models is a good alternative. Apart from being simple, rapid and reproducible, *in vitro* models enable using a broad range of conditions and studying the mechanisms involved in the toxic response.

In intestinal Caco-2 epithelial cells, PTX2 inhibited F-actin polymerisation without affecting cell viability, oxidative stress or cytokine IL-8 release (Ares et al., 2005; Alarcan et al., 2019). Nevertheless, alteration of the intestinal monolayer integrity was pointed out with PTX2 in Caco-2 cells (Hess et al., 2007). In contrast, YTX induced a decrease of cell viability in various intestinal cell lines but without any alteration of F-actin (Ares et al., 2005; Botana et al., 2014; Ferron et al., 2016). Although no increase of oxidative stress and IL-8 release was oberved in Caco-2 cells (Alarcan et al., 2019), YTX affected the intestinal barrier integrity coupled with a degradation of E-cadherin (Ronzitti et al., 2004; Hess et al., 2007). AZA1 triggered disturbance of junction proteins such as occludin and E-cadherin (Abal et al., 2017), indicating an alteration of the intestinal barrier integrity (Hess et al., 2007) even if no alteration of cell morphology was reported in Caco-2 cells (Ronzitti et al., 2007; Abal et al., 2017). AZA1 induced also nucleus and mitochondrial damage, caspases activation and autophagosomes formation in intestinal cells (Twiner et al., 2012; Abal et al., 2017; Bodero et al., 2018). Concerning OA, studies reported a decrease of cell viability in various intestinal cell lines (Blay and Poon, 1995; Ray et al., 2005; Serandour et al., 2012; Ferron et al., 2014; Hayashi et al., 2018) but also activation of caspase-3 and NF-κB as well as cell cycle disturbance (Ferron et al., 2014). Besides, OA increased the paracellular permeability of intestinal cell monolayers (Tripuraneni et al., 1997; Okada et al., 2000; Ehlers et al., 2011; Dietrich et al., 2019).

Surprinsingly, the impact of phycotoxins on mucus secretion has never been investigated *in vitro*. In fact, most of the *in vitro* studies have used only one cell line while the human intestinal epithelium is composed of enterocytes (80-85 %) (Dutton et al., 2019), as well as various other cell types such as endocrine cells, Paneth cells, stem cells, M cells and goblet cells (Berger et al., 2017). Several *in vitro* human intestinal co-culture models combining enterocytes and mucus cells have been developed to mimic the *in vivo* situation. Among them, the co-culture of intestinal Caco-2 enterocytes with HT29-MTX goblet cells has shown a strong polarity with tight and adherens junctions, the presence of a thick mucus layer and permeability values close to human intestine (Beduneau et al., 2014, Ferraretto et al., 2018, Mahler et al., 2009, Pan et al., 2015). Nevertheless, such co-culture model has

never been used for investigating phycotoxins effects on the intestinal barrier. In this context, we evaluated the toxicity of PTX2, YTX, AZA1 and OA on Caco-2/HT29-MTX co-cultures. After 21 days of culture, the Caco-2 cell line differentiates into enterocyte-like cells (Natoli et al., 2012), and the mucus secreting cell line HT29-MTX can mimic goblet cells (Martinez-Maqueda et al., 2015). Cell viability, cellular monolayer integrity, modulation of cell type proportion, production of mucus and inflammation were investigated with various methodologies such as transepithelial electrical resistance (TEER), lucifer yellow (LY) crossing, ELISA, RT-qPCR, periodic acid Schiff and alcian blue (PAS/AB) staining and High Content Analysis (HCA).

2. Materials and Methods

2.1 Chemicals

Cell culture products were purchased from Gibco (Cergy-Pontoise, France). Bovine serum albumin (BSA), Tween 20, Triton, neutral red, LY and HEPES were supplied by Sigma-Aldrich (Saint Quentin Fallavier, France). Monoclonal IL-8, biotinyled monoclonal IL-8 antibodies, SuperBlock blocking buffer, streptavidin peroxidase, TNFα, TMB and paraformaldehyde were purchased from ThermoFisher Scientific (Waltham, MA). For histology, ethanol, toluene, paraffin, Alcian Blue 8GX, Schiff's reagent and Mayer Hematoxylin solution were purchased from VWR (Radnor, PA). Bluing reagent was purschased from Microm (Brignais, France). Pectenotoxin-2, yessotoxin, azaspiracid-1 and okadaic acid, dissolved in methanol (MeOH), were purchased from the National Research Council Canada (NRCC, Halifax, Nova Scotia, Canada).

2.2 Cell culture and toxins exposure

Caco-2 cells (HTB-37) were obtained from the American Type Culture Collection (ATCC) (Manasas, VA), and Caco-2-GFP cells (transfected with EGFP-encoding lentivirus and stably expressing GFP) were kindly provided by Dr. F. Barreau (INSERM IRSD U1220, Toulouse, France). Caco-2 and Caco-2-GFP were maintained in Minimum Essential Medium containing 5.5 mM D-glucose, Earle's salts and 2 mM L-alanyl-glutamine (MEM GlutaMAX) supplemented with 10% fetal bovine serum (FBS), 1% non-essential amino acids, 50 IU/mL penicillin and 50 µg/mL streptomycin at 37°C and 5% CO_2. HT29-MTX were kindly provided by Dr T. Lesuffleur (INSERM U843, Paris, France) and cultured in Dulbecco's Modified Eagle's Medium with high glucose (DMEM) supplemented with 10% inactivated FBS, 50 IU/mL penicillin and 50 µg/mL streptomycin (complete DMEM) at 37°C and 5% CO_2. For subculture, cells were seeded in 75 cm^2 culture flasks and passaged once (for HT29-MTX cells) or twice a week (for Caco-2 cells). For co-culture experiments, Caco-2 and HT29-MTX cells (3:1) were seeded at 157,000 cells/cm^2 in complete DMEM. The ratio (3:1) was selected as it is commonly used for mimicking the proportions found in human tissue (Kleiveland, 2015). 96-well plates were used for cytotoxicity, inflammation (IL-8 release) and immunofluorescence assays, while 12-well and 24-well inserts (polyester membrane, 0.4 µm pore size; Corning, USA) were used for respectively qPCR assays, and for monolayer integrity and histology assays respectively. For identification of the Caco-2 cells in the co-culture, Caco-2-GFP and HT29-MTX cells (3:1) were seeded at 157,000 cells/cm^2 in complete DMEM in 96-well plates. Culture medium was changed three times each week up to 21 days post-seeding. Differentiated co-cultured cells were exposed to toxins in FBS free complete DMEM. A vehicle control (5% MeOH) was included in each experiment.

2.3 Neutral red upatke assay

After 24 hrs of treatment, cytotoxicity was assessed by the neutral red uptake (NRU) assay as previously described (Reale et al., 2019). Absorbance was measured at 540 nm with a microplate reading spectrofluorometer (Fluostar OPTIMA, BMG Labtech, Champigny sur Marne, France). Three independent experiments were performed, and for each experiment, the median of three technical replicates was expressed relative to that of the vehicle control. The IC_{50} was determined using GraphPad Prism Software (version 5.0, GraphPad Software Inc., La Jolla, CA).

2.4 Measurement of IL-8 release

After 24 hrs of treatment, the medium of the 96-well plates used for the cytotoxicity assays was collected for Il-8 measurement. The levels of interleukin-8 (IL-8) released in cell medium were determined as previously described (Tarantini et al., 2015). TNFα (10 nM) was used as positive control. Three independent experiments with three technical replicates per experiment were performed.

2.5 ZO-1 immunofluorescence

After 24 hrs of treatment, the detection of ZO-1 was performed by immunofluorescence as previously described (Ferron et al., 2014) with the following modifications. Antibodies used were anti-rabbit ZO-1 (1/200, ThermoFisher Scientific) and goat anti-rabbit IgG (H+L) Alexa Fluor®647 (1/1000, ab150079, Abcam, Cambridge, UK). Cell identification was performed using DAPI (Sigma-Aldrich) labelling. TNFα (50 nM) was used as positive control for a decrease of ZO-1 protein.. Two independent experiments with three technical replicates per experiment were performed.

2.6 Monolayer integrity assays

2.6.1 TEER measurement

The trans-epithelial electrical resistance (TEER) of the Caco-2/HT29-MTX co-cultured cells was measured to evaluate the monolayer integrity before and after a 24 hrs-treatment with toxins loaded in the apical compartment. For the TEER measurement, assessed with a Millicell Electrical Resistance System supplied by Millipore (Merck, Burlington, MA), the Caco-2/HT29-MTX co-cultured cells were incubated for 30 min at 37°C with 300 and 700 µL transport buffer (HBSS, HEPES 5 mM, pH 7.4) respectively in the apical and basolateral compartments. For each experimental condition, cell-free inserts were included. The TEER value was expressed as ohm.cm² and calculated according to the following equation:

$$TEER = (R_S - R_B) \times A$$

with R_S the resistance value of the Caco-2/HT29-MTX cells monolayer on inserts, R_B the resistance value of the cell-free inserts, and A the insert area (0.33 cm²). Based on our lab historical data, only Caco-2/HT29-MTX cells monolayer with a TEER > 130 ohm.cm² were considered suitable corresponding to a permeability coefficient Papp below 1%/h. Two independent experiments were performed.

2.6.2 LY crossing

The impact of toxins on the Caco-2/HT29-MTX cells monolayer integrity was also evaluated by the ability of LY, a paracellular marker, to cross the Caco-2/HT29-MTX cells monolayer. Following the second TEER measurement, 100 µL of 1 mM LY in transport buffer was loaded in the apical compartment, and the basolateral compartment was filled with 500 µL of transport buffer. The plates were incubated at 37 °C and shaken at 100 rpm on a microplate shaker (Thermo Scientific) for 3 hrs. The basolateral compartment was harvested and fluorescence was measured (excitation at 405 nm, emission at 520 nm) with a microplate reading spectrofluorometer (Fluostar OPTIMA). The amount of LY crossed into the basolateral compartment was expressed relative to that of the initial

amount loaded into the apical compartment, and then expressed per hour. Two independent experiments were performed. A standard curve of LY from 1 μM to 0.01 μM was included.

2.7 Mucus analysis

Following 24 hrs treatment, inserts with Caco-2/HT29-MTX co-cultured cells were washed twice with PBS before removing the membranes from the inserts. After placement in embedding cassettes, membranes were fixed with paraformaldehyde 4% in distilled water for 60 min at room temperature. Dehydration and paraffin embedding of the membranes were performed using an automate (Shandon Cidadelle 100, GMI, Ramsey, MN) as follow: three washes in PBS, ethanol (70% 1 hr, 96% 3 x 2 hrs, and 100% 3 x 2 hrs), toluene (2 x 2 hrs), paraffin (2 x 2 hrs). Histological sections of 4 μm thickness were cut using a Shandon Finesse E+ microtome (ThermoScientific*).* Slides were dewaxed and soaked in xylene (Sigma-Aldrich, Saint Quentin Fallavier, France) for 15 min and then in ethanol 100° for 10 min with an automate LEICA ST 5020 (Leica, Wetzlar, Germany). After staining, images were acquired with a scanner NanooZommer (50× magnification) and analysed with NIS-Element AR Analysis 4.11.00 software. Two independent experiments were performed and, for each independent experiment, the median of three sections was calculated. Slides were coded for blind scoring.

2.7.1 AB staining

Alcian blue (AB) staining was used to visualize acidic mucins. Acidic mucins were stained with 0.1% AB 8GX in 3% glacial acetic acid pH 2.6 for 20 min. After wash with distilled water, nuclei were stained with 0.1% nuclear fast red solution in distilled water for 5 min. Slides were dehydrated in ethanol 100° for 6 min and then in xylene for 4 min.

2.7.2 PAS staining

Periodic Acid Schiff's (PAS) staining was used to visualize neutral mucins. Slides were stained with 1% PAS in distilled water for 5 min, in Schiff's reagent for 12 min and then stained with 10% Mayer Hematoxylin solution and with Bluing reagent for 1.5 min. Slides were dehydrated in ethanol 100° for 6 min and then in xylene for 4 min.

2.8 RT-qPCR

For each toxin, maximal applied concentrations were chosen as IC_{15} according to the NRU assay results. After 24 hrs of treatment with PTX2 (100, 150, and 200 nM), YTX (25, 50, and 100 nM), AZA1 (7.5, 15, and 30 nM) and OA (75, 125, and 175 nM), experiments were performed as previously described (Reale et al., 2019) with the following modifications. Reverse transcription was performed with 2.5 μg of total RNA, and quantitative PCR reactions were carried out with 6.25, 1.56 or 0.39 ng cDNA, depending of the target gene. All primers were purchased from Sigma-Aldrich, and additionnal informations on target genes and oligonucleotide primers are listed in Table S1. Calibration curves were established for each gene from a serial two-fold dilution of a reference sample (pool of cDNA samples). According to these calibration curves, for each sample, mean relative amounts of mRNA of the targeted genes were calculated and then normalized to that of the reference gene. Using NormFinder software, the gene *RPLP0* was chosen as a reference gene since it did not exhibit any significant variation of expression among the samples. The normalized means were used for statistical analyses and values were presented as arbitrary units. Three independent experiments were performed.

2.9 Identification of the Caco-2 cells population in the Caco-2/HT29-MTX co-culture

As PTX2 and OA showed interesting results, we evaluated which cell subpopulation (Caco-2 or HT29-MTX) was affected. After 24 hrs of toxin treatment, Caco-2-GFP/HT29-MTX cells (3:1) were co-incubated at 37 °C for 15 min with 3 μg/mL Hoescht 33342 (Sigma-Aldrich) in complete DMEM.

Fluorescence was monitored with an Arrayscan VTI HCS Reader (Thermo Scientific) associated with a live cell chamber. The Target Activation module of the BioApplication software was used to identify Caco-2-GFP cells. Total cell count was performed using Hoescht labelling. Wells with only Caco-2-GFP cells was used as positive control. Three independent experiments were performed, and for each experimental condition, the number of Caco-2-GFP cells was expressed relative to the total cell number.

2.10 Statistics

GraphPad Prism software was used for statistical analyses. An analysis of variance (ANOVA) was performed, and, when the effect of concentration was significant ($P < 0.05$), the values were compared to the control using the Dunnett's test. Differences were declared significant at $P < 0.05$. The values presented are means ± SEM.

3. Results

3.1. Cytotoxic and morphological effects of phycotoxins

After a 24 hrs treatment, an IC_{50} could only be established for OA (IC_{50} = 550 ± 104 nM) (Figure 1). A slight decrease of cell viability (around 20%) was observed with the highest concentrations for the other toxins (260 nM PTX2, 200 nM YTX and 77 nM AZA1).

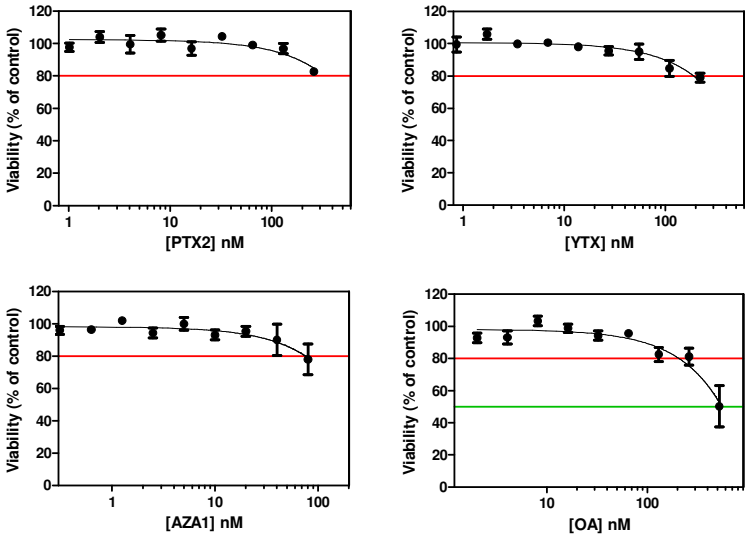

Figure 1. Cytotoxicity on Caco-2/HT29-MTX co-cultured cells after a 24 hrs exposure to PTX2, YTX, AZA1 and OA in 96-well plates. Cytotoxicity was measured by the neutral red uptake (NRU) assay. Red line: 80% of viability; green line: 50% of viability. Values are presented as means ± SEM, and expressed as percentages relative to the vehicle control. Three independent experiments with three technical replicates per experiment were performed.

Cellular morphology was observed after 24 hrs of treatment (Figure 2). While YTX and AZA1 did not induce any morphological changes, treatment with PTX2 and OA showed large areas without cells (above 65 nM PTX2) as well as severe cell rounding (above 130 nM OA).

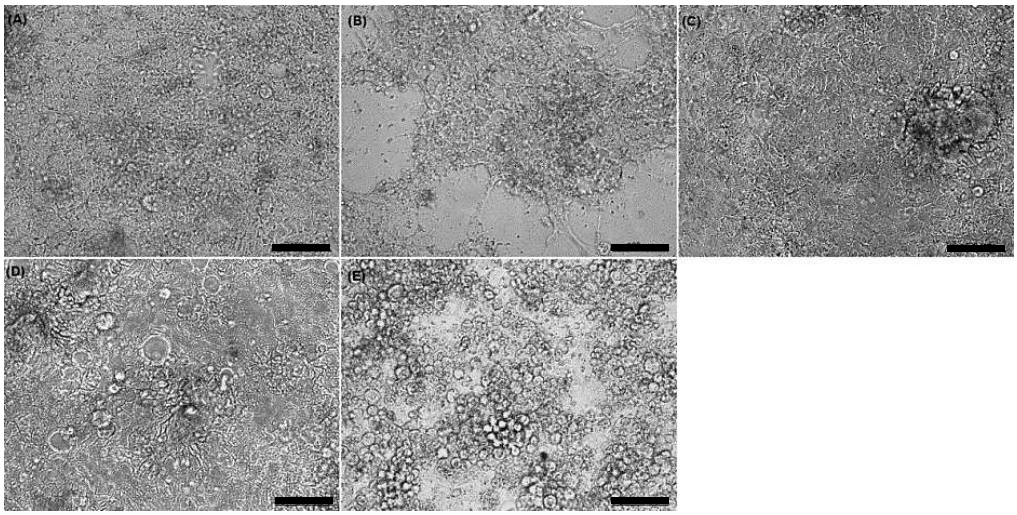

Figure 2. Morphological changes of Caco-2/HT29-MTX co-cultured cells after 24 hrs exposure to PTX2, YTX, AZA1 and OA in 96-well plates. Evaluation of cell morphology was carried out by phase contrast microscopy. Each image is representative of three independent experiments. (A): vehicle control (5% MeOH), (B): 260 nM PTX2, (C): 220 nM YTX, (D): 80 nM AZA1, and (E): 520 nM OA. Scale bar = 100 µm.

3.2. Cellular monolayer integrity

3.2.1 TEER and LY permeability

The TEER value for the vehicle control was on average 162 ± 7.5 ohm.cm² (Figure 3). The integrity of the Caco-2/HT29-MTX cells monolayer was affected after 24 hrs treatment with PTX2 and OA. TEER values decreased significantly reaching -38% with 260 nM PTX2, and -87% with 320 nM OA. A slight but not significant decrease was noticed after exposure to YTX and AZA1.

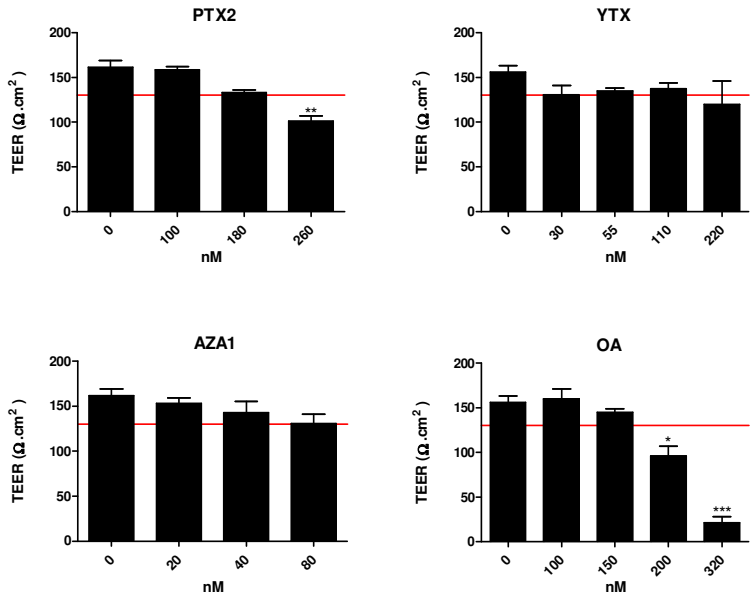

Figure 3. TEER measurement on Caco-2/HT29-MTX co-cultured cells after 24 hrs exposure to PTX2, YTX, AZA1 and OA in 24-well inserts. Red line: 130 ohm.cm². Values are presented as means

± SEM. Two independent experiments with two technical replicates per experiment were performed. *, **, ***: value significantly different from the vehicle control (respectively $P < 0.05$, $P < 0.01$ and $P < 0.001$).

For the vehicle control, the relative amount of LY that crossed into the basolateral compartment was on average 0.400 ± 0.005 %/h (Figure 4). The relative amount of LY crossing the Caco-2/HT29-MTX cells monolayer was significantly increased reaching 9.4, 1.5 and 1.3 %/h at the highest concentration for OA, PTX2 and AZA1 respectively. For YTX, it was difficult to clearly state to an increase of LY crossing due the variability observed at the highest concentration.

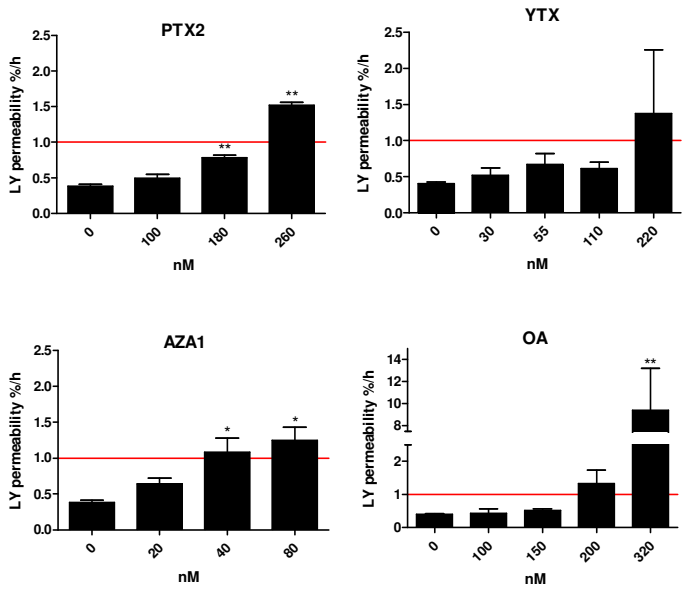

Figure 4. LY crossing through Caco-2/HT29-MTX co-cultured cells after 24 hrs exposure to PTX2, YTX, AZA1 and OA in 24-well inserts. Values are presented as means ± SEM, and expressed as percentage of LY that had crossed into the basolateral compartment per hour. Two independent experiments with two technical replicates per experiment were performed. *, **: value significantly different from the vehicle control (respectively $P < 0.01$ and $P < 0.001$).

3.2.2 ZO-1 immunofluorescence

In the vehicle control, ZO-1 was distributed mainly at the cell border (Figure 5). Irrespective of the toxin, ZO-1 localization was perturbed and redistributed, showing irregular cell borders labelling due to ZO-1 transfer from tight junctions to the cytoplasm. However, these effects were less pronounced with YTX and AZA1. As observed with light microscopy, 260 nM PTX2 and 320 nM OA showed areas without cells.

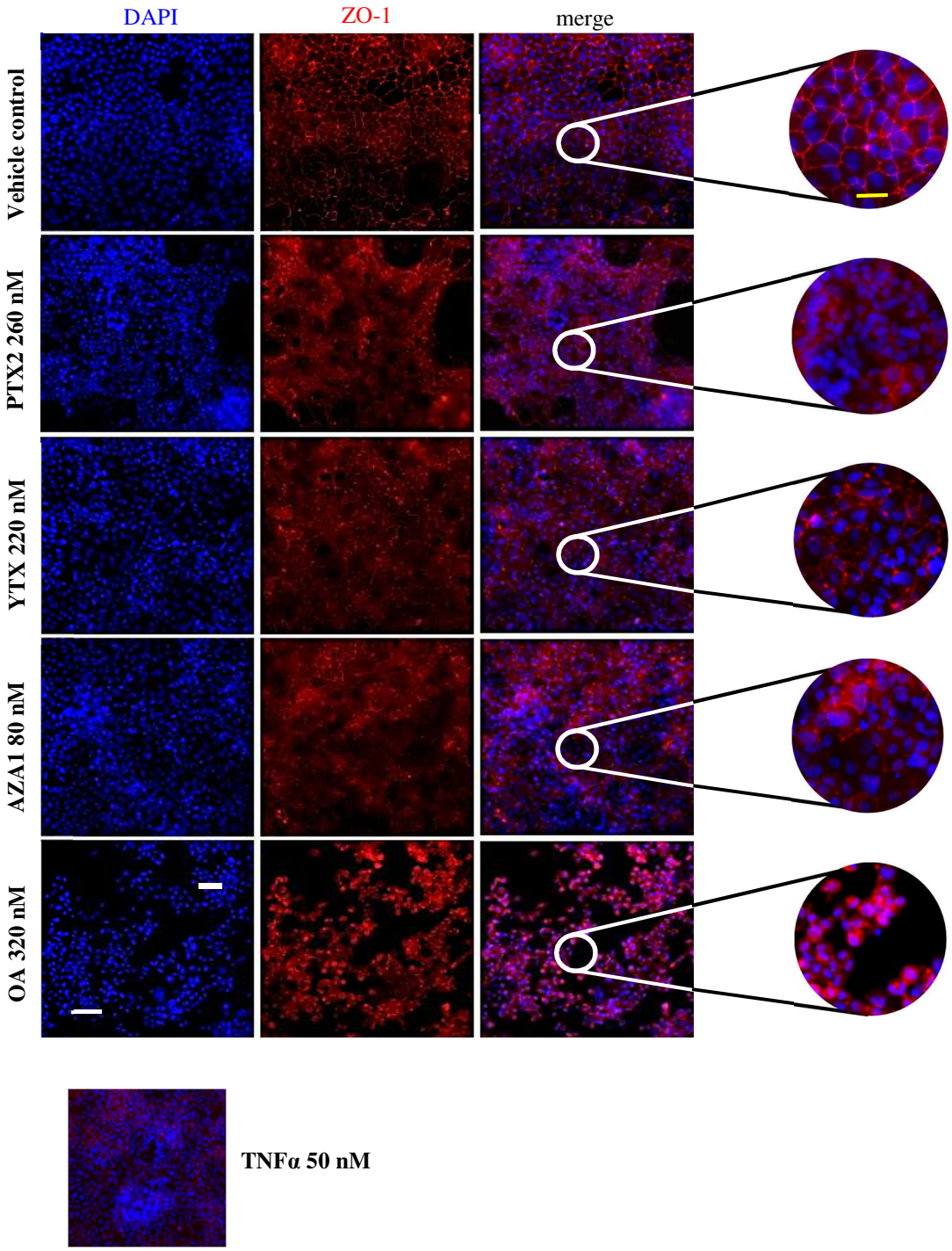

Figure 5. Immunofluorescence localization of zonula occludens (ZO-1) in Caco-2/HT29-MTX co-cultured cells after 24 hrs exposure to PTX2, YTX, AZA1 and OA in 96-well plates. 50 nMTNFα was used as positive control. ZO-1 (red) and DAPI (blue) nucleus staining were carried out by HCA. Each image is representative of two independent experiments. Scale bar = 60 µm (white bar) and 3 µm (yellow bar).

3.3. Inflammatory response

In the vehicle control, the concentration of IL-8 released in the cell medium was on average 73.2 ± 3.3 pg/mL (Figure 6). A concentration dependent increase of IL-8 release was observed after 24 hrs exposure to PTX2 and OA. Compared to the vehicle control, the IL-8 concentration increased significantly up to 3-fold with 260 nM PTX2 and 28-fold with 520 nM OA. No significant modification was pointed out following treatment with YTX up to 220 nM. AZA1 induced a slight but non significant increase of IL-8 release at 40 nM that was no longer observed at the highest concentration (80 nM).

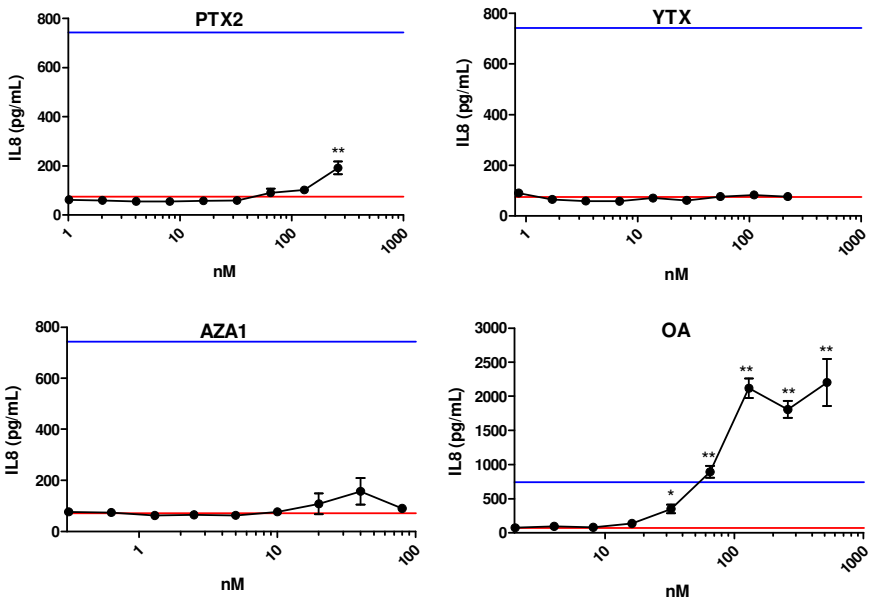

Figure 6. IL-8 release in Caco-2/HT29-MTX co-cultured cells after 24 hrs exposure to PTX2, YTX, AZA1 and OA in 96-well plates. Red line: IL-8 release concentration in the vehicle control (73 pg/mL). Values are presented as means ± SEM. Three independent experiments with three technical replicates per experiment were performed. *, **: value significantly different from the vehicle control (respectively $P < 0.05$ and $P < 0.001$). IL-8 release of the TNFα positive control was 742 ± 7.5 pg/mL (blue line).

3.4. Mucus layer

3.4.1 Acidic mucins

Figure 7A presents the observations by light microscopy of transversal sections of Caco-2/HT29-MTX co-cultures following AB staining. Figure 7B presents the percentage area of AB staining, and the mean intensity of all analyzed blue pixels. PTX2 did not show any significant modification of both acidic mucus area and intensity compared to the vehicle control. YTX, AZA1 and OA induced an increase of AB area of 1.5-, 1.7- and 1.4-fold respectively, although not statistically significant. The increase of mucus area following AZA1 exposure was concomitant with a significant decrease (18%) of AB mean intensity. The two other toxins, YTX and OA, did not affect AB intensity.

(A)

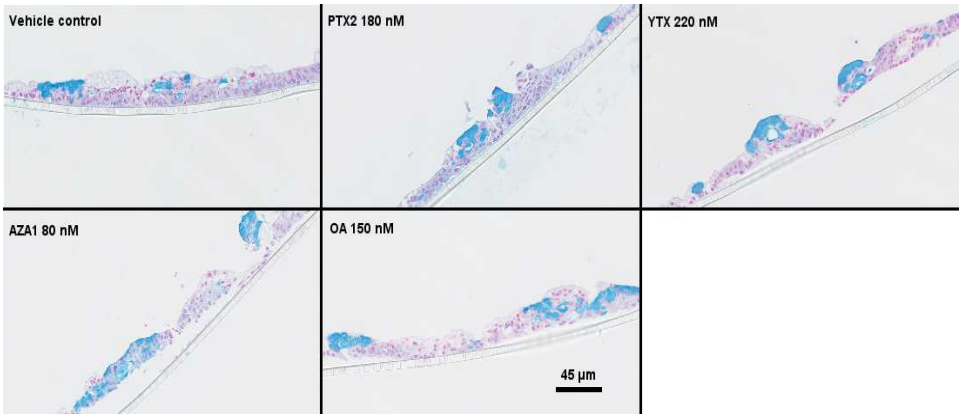

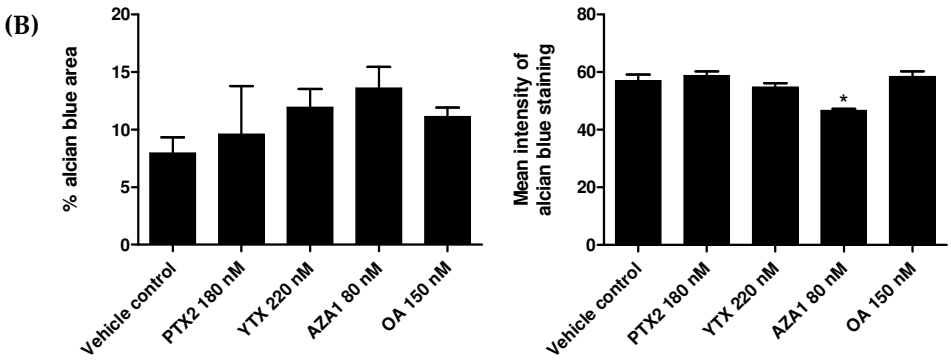

Figure 7. Staining of acidic mucins in Caco-2/HT29-MTX co-cultured cells with alcian blue after 24 hrs exposure to PTX2, YTX, AZA1 and OA in 24-well inserts. (A) Observation by light microscopy of transversal sections. Scale bar = 45 µm. (B) Percentage area of alcian blue staining and mean intensity of all analyzed blue pixels. Values are presented as means ± SEM. Two independent experiments with one technical replicates per experiment were performed. *: value significantly different from the vehicle control ($P < 0.05$).

3.4.2 Neutral mucins

Figure 8A presents the observations by light microscopy of transversal sections of Caco-2/HT29-MTX co-cultures following PAS staining. Figure 8B presents the percentage area of PAS staining, and the mean intensity of all analyzed purple pixels. PTX2 did not show any significant modification of both neutral mucus area and intensity compared to the vehicle control. YTX exposure resulted in an increase of PAS staining area although not statistically significant and without any change of the intensity. A slight, but non-significant, increase of PAS mucus area was observed for OA and AZA1.

(A)

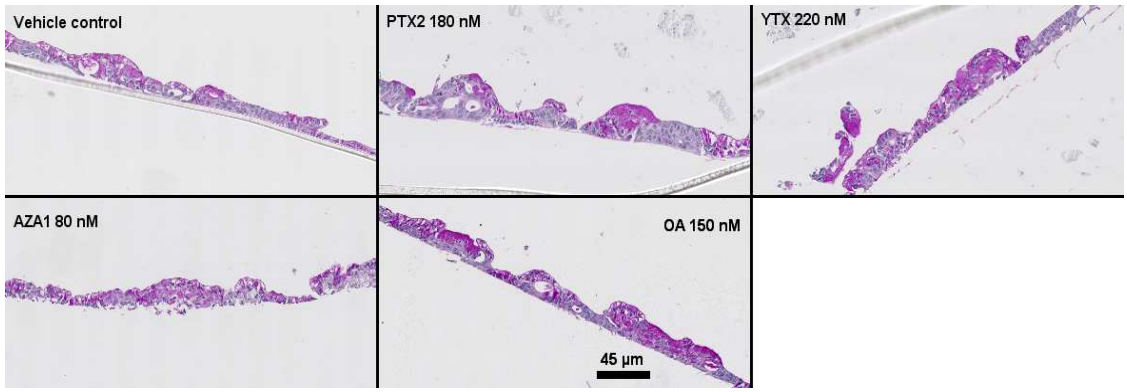

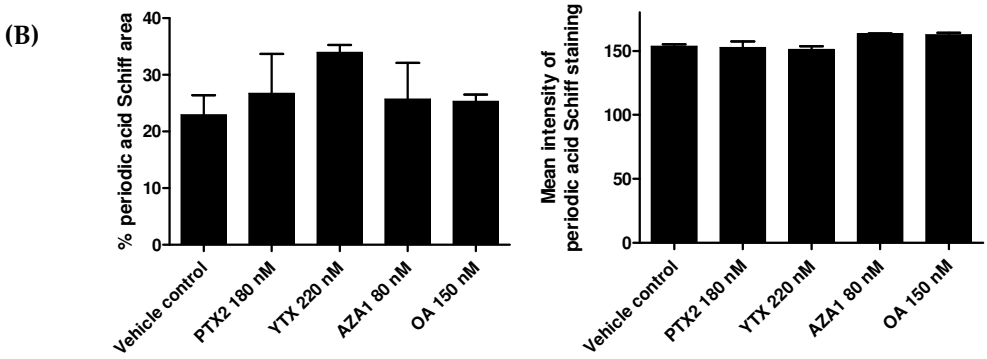

Figure 8. Staining of neutral mucins in Caco-2/HT29-MTX co-cultured cells with periodic acid Schiff after 24 hrs exposure to PTX2, YTX, AZA1 and OA in 24-well inserts. (A) Observation by light microscopy of transversal sections. Scale bar = 45 µm. (B) Percentage area of periodic acid Schiff staining and mean intensity of all analyzed purple pixels. Values are presented as means ± SEM. Two independent experiments with one technical replicates per experiment were performed

3.5. Modulation of gene expression

Additional investigation was done by analyzing some key genes involved in inflammation, adherens and tight junctions, mucus production and channels (Table 1). IC_{15} of each toxin was chosen as maximal concentration. For inflammation, *IL-8* was up regulated for AZA1 (2.9-fold at 15 nM) although not statistically significant. A concentration-dependent up regulation of *IL-8* was observed with OA reaching 7.9-fold at 175 nM. Concerning claudin genes related to adhesion, a concentration-dependent up regulation was observed with 200 nM PTX2 for *CLDN3* (1.6-fold), and also for *CLDN4* (2.8-fold) but not statistically significant. *CLDN4* was also up regulated, but not significantly, with 30 nM AZA1 (2.9-fold) and 175 nM OA (2.5-fold). For mucus, gene expressions of *MUC12* and *MUC13* were significantly up regulated respectively by 200 nM PTX2 (1.7-fold) and 175 nM OA (2.1-fold). A gene implicated in lipid droplet structure (*PLIN2*) was up regulated with OA (1.8-fold at 125 nM) and AZA1 (1.7-fold at 30 nM). This up regulation was concentration-dependent. Except for PTX2, all the toxins induced a significant down regulation of *TFF3* expression ranging from 0.3-fold to 0.5-fold inhibition, the encoded protein being involved in mucosal protection and stabilization of the mucus layer. Regarding channels expression, *AQP3* was significantly down regulated ranging from 0.4-fold to 0.6-fold inhibition in a concentration dependent-manner with all the toxins.

Table 1. Relative gene expression in Caco2/HT29-MTX co-cultured cells after 24 hrs exposure to PTX2, YTX, AZA1 and OA in 12-well inserts. The analysis of gene expression was carried out by RT-qPCR. Values are normalized to the reference gene RPLP0 and presented as fold changes of the vehicle control (red for up-regulated, blue for down-regulated). Three independent experiments with one technical replicates per experiment were performed. *, **, ***: significantly different from the vehicle control (respectively $P < 0.05$, $P < 0.01$ and $P < 0.001$).

Biological functions	Genes	PTX2			YTX			AZA1			OA		
		100 nM	150 nM	200 nM	25 nM	50 nM	100 nM	7.5 nM	15 nM	30 nM	75 nM	125 nM	175 nM
Inflammation	*IL1B*												
	IL8												**
Adherens and tight junctions	*NCT1*												
	OCLN												
	ZO1											*	
	CLD1												
	CLDN3			*									
	CLDN4												
	CDH1												
	CLDN15												
Mucus	*MUC1*												
	MUC12			*									
	MUC13												*
	MUC17												
	MUC5AC												
	MUC5B												
	AGR2												
	TFF1												
	TFF2												
	TFF3				*	*	***	***	**	***		***	***
	PLIN2									**		**	**
	PLIN3												
	B3GNT2												
	B3GALT6												
	B4GALNT3												
	B4GALT5												
	B3GNT5												
	GALNT3												
	GALNT5												
	GALNT1												
	GALNT4												
	GCNT1												
	SNAP23												
	FCGBP												
	CARL												
	UGGT1												
	STX3												
	ERN2												
	OGT												
	VAMP8												
Channel	*CFTR*												
	AQP1												
	AQP3	*	*		***	***	***	**	*	*		*	**
	AQP10												
	DRA												
	ADYC6												
	NKCC1												
Transporter	*ABCG2*												
	ABCC3												
	ABCC2												

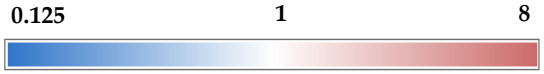

3.6 Evolution of the Caco-2-GFP/HT29-MTX proportion following treatment with PTX2 and OA

After 21 days post-seeding, the Caco-2-GFP/HT29-MTX proportion in the vehicle control was on average 71:29 (Figure 9A). The HT29-MTX cells were mainly aggregated in islets (Figure 9B). The percentage of Caco-2-GFP cells increased significantly after exposure to the toxins, the Caco-2-GFP/HT29-MTX proportion reached 85:15 and 88:12 with 260 nM PTX2 and 320 nM OA respectively concomittantly with a decrease of cell viability. PTX2 treatment provoked the formation of area without cells from 180 nM. Such effects, but weaker, were also observed with OA from 200 nM.

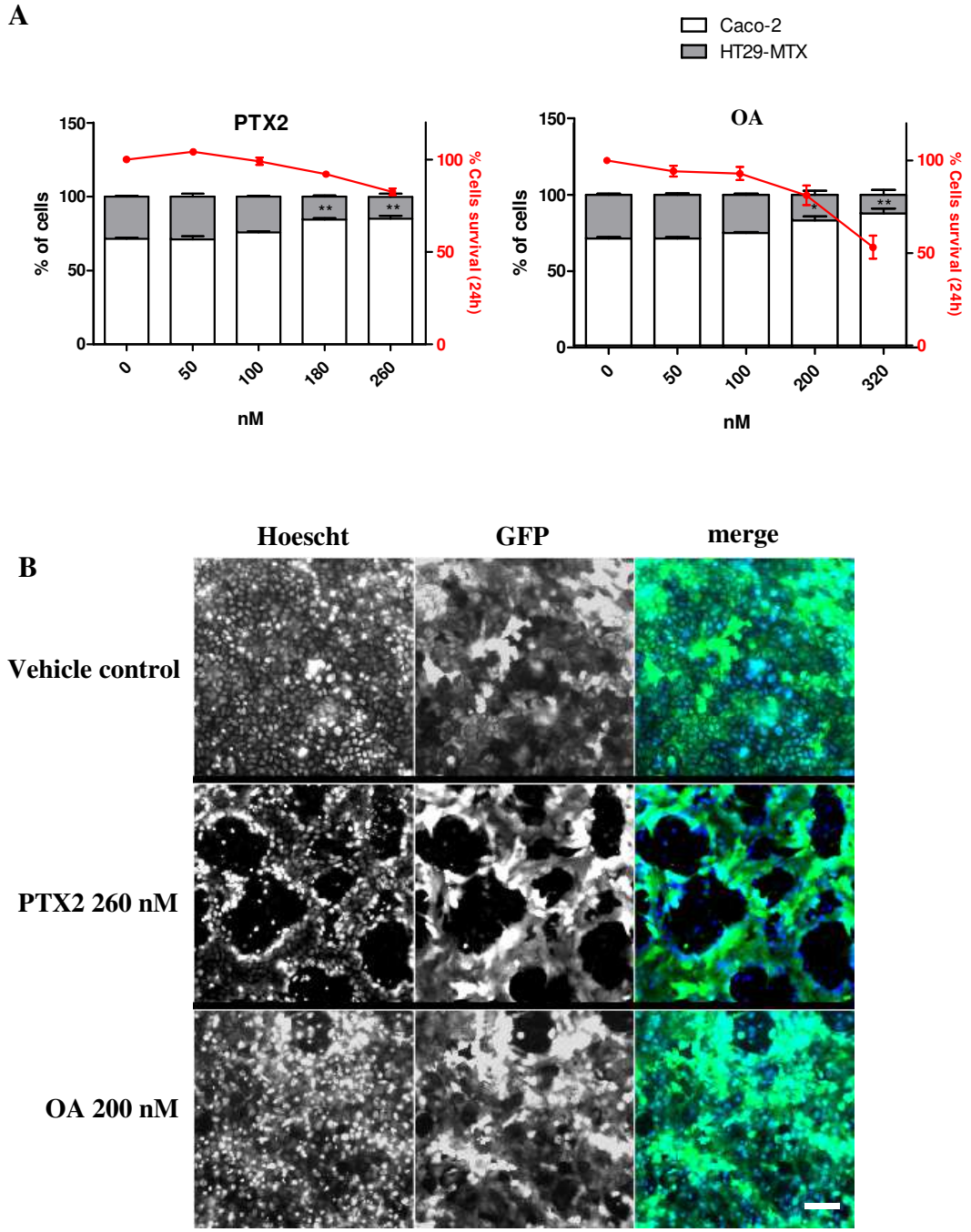

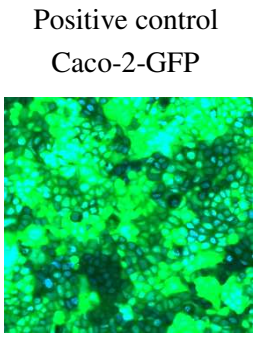

Figure 9. Percentage of Caco-2-GFP and HT29-MTX cells co-cultured after 24 hrs exposure to PTX2 and OA in 96-well plates. Caco-2-GFP cells were identified as green fluorescent cells, and total cell count was determined using Hoescht 33342 labelling. Percentages of each cell line are expressed relative to the total cell number and presented as means ± SEM. Positive control of the full fluorescence represents only Caco-2-GFP. Three independent experiments were performed. *, **: value significantly different from the vehicle control (respectively $P < 0.01$ and $P < 0.001$). Scale bar = 60 µm.

4. Discussion

The Caco-2 and HT29-MTX cell lines represent the two major cell types (absorptive and goblet cells respectively) found in the small intestinal epithelium. In our study, the Caco-2/HT29-MTX cellular monolayer presented a TEER value (around 160 ohm.cm²) much lower than the Caco-2 cells monolayer (400-800 ohm.cm² depending on the cell culture method) (Tor, 2015), but closer to the value measured in human intestine (approximately 40 ohm.cm²) (Ferrec et al., 2001; Takenaka et al., 2014).

Contrary to PTX2 and OA, no significant morphological changes were observed with YTX and AZA1. Nevertheless, a slight decrease of viability (around 20%) was observed with PTX2, YTX and AZA1 at the highest concentrations, reaching even up to 50% for OA. Concerning PTX2, our results on cells proportion showed that HT29-MTX cells are probably more sensitive than Caco-2 cells. This indicated that the slight decrease of viability observed for the Caco-2/HT29-MTX co-cultured cells with PTX2 might be mostly due to an effect on the HT29-MTX cell population. In fact, it has been documented that phase I enzymes play a role in PTX2 detoxification (Alarcan et al., 2017, Ferron et al., 2016b). As HT29-MTX cells do not express CYP (Carrière et al., 1994; Gervot et al., 1996; Mahler et al., 2009; Barlovatz-Meimon and Ronot, 2014), this may explain the greater sensitivity of HT29-MTX cells to PTX2 compared to Caco-2 cells. In contrast, a decrease of viability (around 20%) was reported in differentiated Caco-2 cells exposed to 200 nM PTX2 (Alarcan et al., 2019), indicating that Caco-2 cells alone seem to be more sensitive to PTX2 than in co-culture with HT29-MTX cells. Although we do not have a clear explanation for that, the mucus layer may be involved in protecting the cells. Additional studies will be necessary to verify this hypothesis. Surprisingly, YTX exposure showed a different toxicity profile with a slight decrease of the Caco-2/HT29-MTX co-cultured cells viability while no effect was observed on differentiated Caco-2 cells alone up to 200 nM YTX (Alarcan et al., 2019). This discrepancy could be related to the viability test performed: as YTX is known to disrupt lysosomes (Malagoli et al., 2006), the NRU assay (detecting lysosome activity), used in our study, is certainly more sensitive than cell counting to depict YTX toxicity. While no cytotoxicity in

differentiated Caco-2 cells was reported up to 72 hrs with 500 nM AZA1 (Ryan et al., 2004; Hess et al., 2007; Vilarino et al., 2008; Abal et al., 2017), we observed a slight decrease of viability in Caco-2/HT29-MTX co-cultured cells. Compared to the three phycotoxins mentioned above, OA cytotoxicity and kinetics data on intestinal cells have been extensively published. IC_{50} ranged from 200 to 400 nM after 24 hrs of exposure on differentiated Caco-2 cells (Ehlers et al., 2011; Alarcan et al., 2019; Dietrich et al., 2019), suggesting a higher sensitivity of the Caco-2 cells cultured alone than in co-culture with HT29-MTX cells (IC_{50} = 550 nM). Once again, the presence of the mucus layer may protect Caco-2 cells against OA. Similarly to PTX2, HT29-MTX cells seem to be more sensitive to OA than Caco-2 cells (as suggested by the decrease of HT29-MTX cells percentage in the co-culture). Indeed, the higher sensitivity of non-differentiated HT29-MTX cells compared to non-differentiated Caco-2 cells to OA was shown by Ferron et al (2014). Again, a higher detoxification of OA by Caco-2 cells through P-gP and CYP activity (Ehlers et al., 2014; Kittler et al., 2014; Ferron et al., 2016b) cannot be excluded. Therefore, the two cell types showed an obvious difference in sensitivity to toxins that may be driven by their own detoxification capacities.

For Caco-2/HT29-MTX co-cultured cells, two toxins induced a concentration-dependent alteration of the two markers of monolayer integrity (a decrease of TEER values correlated with an increase of LY crossing). For PTX2, concomitantly to a decrease of TEER, a decrease of *CLD1* expression and a cytoplasmic redistribution of ZO-1 were observed at the highest concentration. This is consistent with PTX2 targeting F-actin (Espina et al., 2008). Our results of TEER and LY crossing indicated that OA up to 150 nM did not affect the Caco-2/HT29-MTX monolayer integrity, in accordance with other studies performed on Caco-2 cells monolayer (Ehlers et al., 2011; Fernandez et al., 2014). For OA concentrations above 150 nM, alteration of the monolayer integrity was linked to morphological changes (rapid swelling and cell rounding and the formation of areas without cells (figures 2 and 5). We also observed a cytoplasmic redistribution of ZO-1, a tight-junction protein commonly used for investigating the effect of compounds on intestinal barrier integrity. A slight down-regulation of the tight junction *CLD1* gene was also induced by OA. Similarly, a decrease of both gene expression and proteins levels of tight junction proteins has been already described in differentiated Caco-2 cells exposed to 150 nM OA (Dietrich et al., 2019). A cytoplasmic redistribution of ZO-1 has been also reported in mouse mammary epithelia 31EG4 cells exposed to OA (Singer et al., 1994). AZA1 induced some alteration of permeability observed by a slight increase of LY crossing while YTX did not significantly affect monolayer permeability. In contrast, moderate (Abal et al., 2017) to strong (Hess et al., 2007) decrease of TEER was reported for Caco-2 cells exposed up to 100 nM AZA1. Although we did not observe much cytoplasmic redistribution of ZO-1 in Caco-2/HT29-MTX co-cultured cells treated with AZA1, modification of the distribution of other tight junction components, such as occludin and E-cadherin, has been reported in differentiated Caco-2 cells (Bellocci et al., 2010; Abal et al., 2017). Even if a decrease of *AQP3* expression has been shown to be correlated with a decrease of TEER, occludin and claudin-1 expressions (Zhang et al., 2011; Ikarashi et al., 2016; Ikarashi et al., 2019), in our study, YTX strongly decreased the *AQP3* expression without modification of the TEER values. In contrast, the down-regulation of *AQP3* was weaker for OA, although an increase of permeability was observed. Thereby, we did not find that *AQP3* expression

and TEER were strongly correlated, and the discrepancy with the literature data requires further investigation.

Other parameters such as inflammation mediators can be involved in the alteration of the Caco-2/HT29-MTX monolayer integrity (Sedgwick et al., 2002). Indeed, inflammation has been shown to be involved in the alteration of intestinal cells monolayer integrity, particularly through the release of IL-8, IL-1β (Al-Sadi et al., 2008), TNFα (Ma et al., 2004; Al-Sadi et al., 2016) and IFNγ (Beaurepaire et al., 2009). Therefore, we have evaluated if the decrease of Caco-2/HT29-MTX monolayer integrity could be linked to IL-8 release, a marker of inflammation commonly used for investigating phycotoxins toxicity on intestinal cell lines (Alarcan et al., 2019, Ferron et al., 2016c). In this co-culture model in 96-well plates, the basal level of IL-8 release was very close to that of Caco-2 cells alone (Alarcan et al., 2019). We observed that OA exposure induced a large increase of IL-8 expression and protein release. Similarly, an increase of IL-8 release (around 30-fold) has been reported in differentiated Caco-2 cells exposed to OA but at a lower concentration (38 nM) (Alarcan et al., 2019). As already suggested for viability results, the mucus layer produced in co-cultures may protect Caco-2 cells against OA toxicity, leading to IL-8 release with higher OA concentrations compared to Caco-2 cells alone (Alarcan et al., 2019). The inflammatory response (IL-8 release) was in accordance with NF-κB translocation observed following OA treatment in intestinal epithelial and glial cells (Ferron et al., 2014; Reale et al., 2019). NF-κB is involved in inflammation as precursor of cytokines release as well as in gut homeostasis (Gupta et al., 2010).

With PTX2, we observed a slight increase in IL-8 release only at the highest concentration tested (260 nM) (Figure 6). This response was not supported by an increase of IL-8 gene expression that, in contrast, was slightly -but non-significantly- down-regulated. In agreement with our observations, no IL-8 release was reported previously in differentiated Caco-2 cells treated with 200 nM PTX2 (Alarcan et al., 2019). Finally, the absence of effect on IL-8 release and gene expression after exposure of Caco-2/HT29-MTX co-cultured cells to YTX is consistent with the results reported in differentiated Caco-2 cells (Alarcan et al., 2019). Still, no study has investigated the effect of AZA1 on inflammation in intestinal cells. However, *in vivo* studies on rodents exposed to YTX or AZA1 pointed out the presence of infiltrated lymphocytes, reflecting an inflammatory area in the gut submucosa (Franchini et al., 2010), the presence of neutrophils in the lamina propria (Aune et al., 2012; Kilcoyne et al., 2014) as well as the infiltration of inflammatory cells in lung and liver (Ito et al., 2002). Therefore, it could be suggested that the inflammatory response observed in rodents was driven by another pathway than IL-8 or by another cell type than enterocytes or goblet cells.

Both acute stress and cytokines release, such as IL-8, can stimulate mucus secretion (Hansvall and Ianowski, 2014, Hart and Kamm, 2002). Surprisingly, the impact of phycotoxins on the intestinal mucus production *in vitro* has never been evaluated. In Caco-2/HT29-MTX co-cultured cells, OA slightly increased the expression of *MUC13*, a transmembrane mucin, as well as *PLIN2*, a gene involved in lipid droplet structure for mucins. Lipid droplets transport mucins from the intracellular compartment to the apical side of goblet cells. Evaluation of mucus staining showed a slight increase of acidic mucins area at 150 nM OA, although not significant. In fact, the mucus increase is expected to reflect mainly the response of HT29-MTX cells to toxins. Therefore, although the percentage of

HT29-MTX cells was not affected until 200 nM OA, the low percentage of HT29-MTX cells in the co-culture could explain why the response on mucus was not significant. In co-cultures, it is not excluded that the secretion of cytokines/chemokines by Caco-2 cells stimulates HT29-MTX cells resulting in an inflammatory response and perhaps mucus secretion. For PTX2, although the AB and PAS stainings did not reveal any significant modification of mucus area, a slight increase of MUC12 was observed at the highest concentration, concomitantly with a decrease of HT29-MTX cell population. In contrast, YTX and AZA1 did not affect mucins expression but a slight increase of the acidic and neutral mucins area was observed at 80 nM AZA1 and 220 nM YTX respectively. Therefore, it could be worth measuring mucus production of HT29-MTX cells alone in response to phycotoxins exposure. Moreover, post-transcriptional O-glycosylation and N-glycosylation of the mucins could be also a pathway to investigate as the aberrant glycan structure of mucins induces perturbation of the gut functions and gut homeostasis (Bergstrom and Xia, 2013; Hanson and Hollingsworth, 2016; Arike et al., 2017).

5. Conclusions

In conclusion, our study investigated the mode of action of 4 phycotoxins using a co-culture intestinal model composed of enterocytes-like (Caco-2) and mucus producing cells (HT29-MTX). We explored how the responses of such model fit with the observations in humans and rodents. Our results indicated that the mucus layer could protect Caco-2 cells from OA toxicity. The HT29-MTX cell population appeared more sensitive to OA and PTX2 than Caco-2 cells. In contrast, YTX and AZA1 induced a slight cytotoxicity, expressed mainly by a slight decrease of monolayer integrity. Our study highlighted that intestinal cell models integrating different cell types may contribute to improve hazard assessment and to describe how phycotoxins can affect human intestinal tract. Therefore, the Caco-2/HT29-MTX is a suitable cell model combining the two major epithelial cells for the evaluation of phycotoxins toxicity on the intestinal barrier. Nevertheless, it does not contain cell types from immune and nervous systems that are also known as key players in the toxic response of food contaminants. Although more complex cell models are developed to integrate such cell types, they are still not validated to replace *in vivo* studies.

Author Contributions: Conceived and designed the experiments: OR, AH, VF. Performed the experiments: OR. Analyzed the data: OR, AH, VF. Wrote the paper: OR, AH, VF.

Acknowledgements: We thank Gérard Jarry (ANSES Laboratory Fougères) and Alain Fautrel (University Rennes 1, US18, UMS 3480 Biosit, Biogenouest, Core Facility H2P2) for their support in histology.

Conflicts of Interest: The authors declare no conflict of interest

References

Aasen, J.A., Espenes, A., Hess, P., Aune, T., 2010. Sub-lethal dosing of azaspiracid-1 in female NMRI mice. Toxicon 56, 1419-1425.

Aasen, J.A., Espenes, A., Miles, C.O., Samdal, I.A., Hess, P., Aune, T., 2011. Combined oral toxicity of azaspiracid-1 and yessotoxin in female NMRI mice. Toxicon 57, 909-917.

571 Abal, P., Louzao, M.C., Fraga, M., Vilarino, N., Ferreiro, S., Vieytes, M.R., Botana, L.M., 2017. Absorption and
572 Effect of Azaspiracid-1 Over the Human Intestinal Barrier. Cell Physiol Biochem 43, 136-146.

573 Al-Sadi, R., Guo, S., Ye, D., Rawat, M., Y. Ma, T., 2016. TNF-α Modulation of Intestinal Tight Junction
574 Permeability Is Mediated by NIK/IKK-α Axis Activation of the Canonical NF-κB Pathway. Am J Pathol 186,
575 1151-1165.

576 Al-Sadi, R., Ye, D., Dokladny, K., Ma, T., 2008. Mechanism of IL-1b-Induced Increase in Intestinal Epithelial
577 Tight Junction Permeability. The Journal of Immunology 178, 4641–4649.

578 Alarcan, J., Barbe, S., Kopp, B., Hessel-Pras, S., Braeuning, A., Lampen, A., Le Hegarat, L., Fessard, V., 2019.
579 Combined effects of okadaic acid and pectenotoxin-2, 13-desmethylspirolide C or yessotoxin in human
580 intestinal Caco-2cells. Chemosphere 228, 139-148.

581 Alarcan, J., Dubreil, E., Huguet, A., Hurtaud-Pessel, D., Hessel-Pras, S., Lampen, A., Fessard, V., Le Hegarat, L.,
582 2017. Metabolism of the Marine Phycotoxin PTX-2 and Its Effects on Hepatic Xenobiotic Metabolism: Activation
583 of Nuclear Receptors and Modulation of the Phase I Cytochrome P450. Toxins (Basel) 9.

584 Ares, I.R., Louzao, M.C., Vieytes, M.R., Yasumoto, T., Botana, L.M., 2005. Actin cytoskeleton of rabbit intestinal
585 cells is a target for potent marine phycotoxins. J Exp Biol 208, 4345-4354.

586 Arike, L., Holmen-Larsson, J., Hansson, G.C., 2017. Intestinal Muc2 mucin O-glycosylation is affected by
587 microbiota and regulated by differential expression of glycosyltranferases. Glycobiology 27, 318-328.

588 Aune, T., Espenes, A., Aasen, J.A., Quilliam, M.A., Hess, P., Larsen, S., 2012. Study of possible combined toxic
589 effects of azaspiracid-1 and okadaic acid in mice via the oral route. Toxicon 60, 895-906.

590 Aune, T., Sorby, R., Yasumoto, T., Ramstad, H., Landsverk, T., 2002. Comparison of oral and intraperitoneal
591 toxicity of yessotin towards mice. Toxicon 40, 77-82.

592 Barlovatz-Meimon, G., Ronot, X., 2014. Culture de cellules animales-3ème ed. chapitre 27. Système intestinal.

593 Beaurepaire, C., Smyth, D., McKay, D., 2009. Interferon-γ Regulation of Intestinal Epithelial Permeability.
594 Journal of Interferon & Cytokine Research 29.

595 Beduneau, A., Tempesta, C., Fimbel, S., Pellequer, Y., Jannin, V., Demarne, F., Lamprecht, A., 2014. A tunable
596 Caco-2/HT29-MTX co-culture model mimicking variable permeabilities of the human intestine obtained by an
597 original seeding procedure. Eur J Pharm Biopharm 87, 290-298.

598 Bellocci, M., Sala, G.L., Callegari, F., Rossini, G.P., 2010. Azaspiracid-1 inhibits endocytosis of plasma membrane
599 proteins in epithelial cells. Toxicol Sci 117, 109-121.

600 Berger, E., Nassra, M., Atgie, C., Plaisancie, P., Geloen, A., 2017. Oleic Acid Uptake Reveals the Rescued
601 Enterocyte Phenotype of Colon Cancer Caco-2 by HT29-MTX Cells in Co-Culture Mode. Int J Mol Sci 18.

602 Bergstrom, K.S., Xia, L., 2013. Mucin-type O-glycans and their roles in intestinal homeostasis. Glycobiology 23,
603 1026-1037.

604 Blay, J., Poon, A., 1995. Use of cultured permanent lines of intestinal epithelial cells for the assay of okadaic acid
605 in mussel homogenates. Toxicon 33, 739-746.

606 Bodero, M., Hoogenboom, R., Bovee, T.F.H., Portier, L., de Haan, L., Peijnenburg, A., Hendriksen, P.J.M., 2018.
607 Whole genome mRNA transcriptomics analysis reveals different modes of action of the diarrheic shellfish
608 poisons okadaic acid and dinophysis toxin-1 versus azaspiracid-1 in Caco-2 cells. Toxicol In Vitro 46, 102-112.

609 Botana, L.M., Alfonso, A., Vale, C., Vilariño, N., Rubiolo, J., Alonso, E., Cagide, E., 2014. The Mechanistic
610 Complexities of Phycotoxins. pp. 1-33.

611 Callegari, F., Sosa, S., Ferrari, S., Soranzo, M.R., Pierotti, S., Yasumoto, T., Tubaro, A., Rossini, G.P., 2006. Oral
612 administration of yessotoxin stabilizes E-cadherin in mouse colon. Toxicology 227, 145-155.

613 Capaldo, C.T., Nusrat, A., 2009. Cytokine regulation of tight junctions. Biochim Biophys Acta 1788, 864-871.

614 Carrière, V., Lesuffleur, T., Barbat, A., Rousset, M., Dussaulx, E., Costet, P., De Waziers, I., Beaune, P.H.,
615 Zweibaum, A., 1994. Expression of cytochrome P-450 3A in HT29-MTX cells and Caco-2 clone TC7. FEBS Letters
616 355, 247-250.

617 Dietrich, J., Grass, I., Gunzel, D., Herek, S., Braeuning, A., Lampen, A., Hessel-Pras, S., 2019. The marine
618 biotoxin okadaic acid affects intestinal tight junction proteins in human intestinal cells. Toxicol In Vitro 58,
619 150-160.

620 Dominguez, H.J., Paz, B., Daranas, A.H., Norte, M., Franco, J.M., Fernandez, J.J., 2010. Dinoflagellate polyether
621 within the yessotoxin, pectenotoxin and okadaic acid toxin groups: characterization, analysis and human health
622 implications. Toxicon 56, 191-217.

623 Dutton, J.S., Hinman, S.S., Kim, R., Wang, Y., Allbritton, N.L., 2019. Primary Cell-Derived Intestinal Models:
624 Recapitulating Physiology. Trends Biotechnol 37, 744-760.

625 EFSA, 2008. Marine biotoxins in shellfish – Yessotoxin group The EFSA Journal 907, 1-62.

626 EFSA, 2009. Marine biotoxins in shellfish – Pectenotoxin group. The EFSA Journal 1109, 1-47.

627 Ehlers, A., Scholz, J., These, A., Hessel, S., Preiss-Weigert, A., Lampen, A., 2011. Analysis of the passage of the
628 marine biotoxin okadaic acid through an in vitro human gut barrier. Toxicology 279, 196-202.

629 Ehlers, A., These, A., Hessel, S., Preiss-Weigert, A., Lampen, A., 2014. Active elimination of the marine biotoxin
630 okadaic acid by P-glycoprotein through an in vitro gastrointestinal barrier. Toxicol Lett 225, 311-317.

631 Espina, B., Louzao, M.C., Ares, I.R., Cagide, E., Vieytes, M.R., Vega, F.V., Rubiolo, J.A., Miles, C.O., Suzuki, T.,
632 Yasumoto, T., Botana, L.M., 2008. Cytoskeletal toxicity of pectenotoxins in hepatic cells. Br J Pharmacol 155,
633 934-944.

634 Fernandez, D.A., Louzao, M.C., Fraga, M., Vilarino, N., Vieytes, M.R., Botana, L.M., 2014. Experimental basis for
635 the high oral toxicity of dinophysistoxin 1: a comparative study of DSP. Toxins (Basel) 6, 211-228.

636 Ferraretto, A., Bottani, M., De Luca, P., Cornaghi, L., Arnaboldi, F., Maggioni, M., Fiorilli, A., Donetti, E., 2018.
637 Morphofunctional properties of a differentiated Caco2/HT-29 co-culture as an in vitro model of human
638 intestinal epithelium. Biosci Rep 38.

639 Ferrec, E.L., Chesne, C., Artusson, P., Brayden, D., Fabre, G., Gires, P., Guillou, F., Rousset, M., Rubas, W.,
640 Scarino, M.-L., 2001. In VitroModels of the Intestinal Barrier The Report and Recommendations of ECVAM
641 Workshop 29, 649-668.

642 Ferron, P.J., Dumazeau, K., Beaulieu, J.F., Le Hegarat, L., Fessard, V., 2016. Combined Effects of Lipophilic
643 Phycotoxins (Okadaic Acid, Azapsiracid-1 and Yessotoxin) on Human Intestinal Cells Models. Toxins (Basel) 8,
644 50.

645 Ferron, P.J., Hogeveen, K., De Sousa, G., Rahmani, R., Dubreil, E., Fessard, V., Le Hegarat, L, 2016b. Modulation
646 of CYP3A4 activity alters the cytotoxicity of lipophilic phycotoxins in human hepatic HepaRG cells. Tox. In
647 Vitro, 33, 136–146.

648 Ferron, P.J., Lanceleur, R., Diogene, J., Fessard, V., 2016c. Toxicity of palytoxin and Ostreopsis extracts on
649 intestinal, liver, and lung human cells. GdR PHYCOTOX, Villefranche sur Mer.

650 Ferron, P.J., Hogeveen, K., Fessard, V., Le Hegarat, L., 2014. Comparative analysis of the cytotoxic effects of
651 okadaic acid-group toxins on human intestinal cell lines. Mar Drugs 12, 4616-4634.

652 Franchini, A., Malagoli, D., Ottaviani, E., 2010. Targets and Effects of Yessotoxin, Okadaic Acid and Palytoxin:
653 A Differential Review. Marine Drugs 8, 658-677.

654 Fu, L.L., Zhao, X.Y., Ji, L.D., Xu, J., 2019. Okadaic acid (OA): Toxicity, detection and detoxification. Toxicon 160,
655 1-7.

656 Gervot, L., Carrière, V., Costet, P., Cugnenc, P.H., Berger, A., Beaune, P.H., de Waziers, I., 1996. CYP3A5 is the
657 major cytochrome P450 3A expressed in human colon and colonic cell lines. Environmental Toxicology and
658 Pharmacology 2, 381-388.

659 Gupta, S.C.; Sundaram, C.; Reuter, S.; Aggarwal, B.B. Inhibiting NF-kappaB activation by small molecules as
660 a therapeutic strategy. Biochim. Biophys. Acta 2010, 1799, 775–787.

661 Hanson, R.L., Hollingsworth, M.A., 2016. Functional Consequences of Differential O-glycosylation of MUC1,
662 MUC4, and MUC16 (Downstream Effects on Signaling). Biomolecules 6.

663 Hansvall, H., Ianowski, J., 2014. Interleukin-8 stimulates CFTR-mediated mucus secretion by submucosal
664 glands in swine. The FASEB Journal 28.

665 Hart, A., Kamm, M.A., 2002. Review article: mechanisms of initiation and perpetuation of gut inflammation by
666 stress. Aliment Pharmacol Ther 16, 2017-2028.

667 Hayashi, A., Jose Dorantes-Aranda, J., Bowman, J.P., Hallegraeff, G., 2018. Combined Cytotoxicity of the
668 Phycotoxin Okadaic Acid and Mycotoxins on Intestinal and Neuroblastoma Human Cell Models. Toxins (Basel)
669 10.

Hess, P., McCarron, P., Rehmann, N., Kilcoyne, J., McMahon, T., Ryan, G., Ryan, P.M., Twiner, M.J., Doucette, G.J., M., S., Ito, E., Yasumoto, T., 2007. Isolation and purification of azaspiracids from naturally contaminated materials, and evaluation of their toxicological effects– final project report ASTOX (ST/02/02). Marine Institute – Marine Environment & Health 28, 119.

Ikarashi, N., Kon, R., Sugiyama, K., 2016. Aquaporins in the Colon as a New Therapeutic Target in Diarrhea and Constipation. Int J Mol Sci 17.

Ikarashi, N., Nagoya, C., Kon, R., Kitaoka, S., Kajiwara, S., Saito, M., Kawabata, A., Ochiai, W., Sugiyama, K., 2019. Changes in the expression of Aquaporin-3 in the gastrointestinal tract affect drug absorption. International Journal of Molecular Sciences 20, 1-15.

Ishige, M., Satoh, N., Yasumoto, T., 1988. Pathological studies on mice administered with the causative agent of diarrhetic shellfish poisoning (okadaic acid and pectenotoxin-2). Hokkaidoritsu Eisei Kenkyushoho 38, 15-18.

Ito, E., 2006. Abstract PO 08-01. 12th International Conference on Harmful Algae. 198.

Ito, E., Satake, M., Ofuji, K., Higashi, M., Harigaya, K., McMahon, T., Yasumoto, T., 2002. Chronic effects in mice caused by oral administration of sublethal doses of azaspiracid, a new marine toxin isolated from mussels. Toxicon 40, 193-203.

Ito, E., Satake, M., Ofuji, K., N., K., McMahon, T., James, K.J., Yasumoto, T., 2000. Multiple organ damage caused by a new toxin azaspiracid, isolated from mussels produced in Ireland. Toxicon 38, 917-930.

Ito, E., Suzuki, T., Oshima, Y., Yasumoto, T., 2008. Studies of diarrhetic activity on pectenotoxin-6 in the mouse and rat. Toxicon 51, 707-716.

Khora, S.S., Jal, S., 2018. Occurrence of natural toxins in seafood. Microbial Contamination and Food Degradation Chapter 7, 177-233.

Kilcoyne, J., Jauffrais, T., Twiner, M., Doucette, G., Aasen Bunæ, J., Sosa, S., Krock, B., Séchet, V., Nulty, C., Salas, R., Clarks, D., Geraghty, J., Duffy, C., Foley, B., John, U., A. Quilliam, M., McCarron, P., O. Miles, C., Silke, J., Cembella, A., Tillmann, U., Hess, P., 2014. AZASPIRACIDS - Toxicological Evaluation, Test Methods and Identification of the Source Organisms (ASTOX II). in: Series, M.R.S.-P.N.-. (Ed.).

Kittler, K., Fessard, V., Maul, R., Hurtaud-Pessel, D., 2014. CYP3A4 activity reduces the cytotoxic effects of okadaic acid in HepaRG cells. Archives of Toxicology 88, 1519-1526.

Kleiveland, C.R., 2015. Chapter 13 : Co-cultivation of Caco-2 and HT29MTX, The impact of food bioactives on Health - In vitro and Ex vivo models

Lago, J., Santaclara, F., Vieites, J.M., Cabado, A.G., 2005. Collapse of mitochondrial membrane potential and caspases activation are early events in okadaic acid-treated Caco-2 cells. Toxicon 46, 579-586.

Ma, T., Iwamoto, G., Hoa, N., Akotia, V., Pedram, A., Boivin, M., Said, H., 2004. TNF-a-induced increase in intestinal epithelial tight junction permeability requires NF-⊚B activation. Am J Physiol Gastrointest Liver Physiol 286, 367–376.

704 Mahler, G.J., Shuler, M.L., Glahn, R.P., 2009. Characterization of Caco-2 and HT29-MTX cocultures in an in vitro
705 digestion/cell culture model used to predict iron bioavailability. Journal of Nutritional Biochemistry 20, 494-502.

706 Malagoli, D., Marchesini, E., Ottaviani, E., 2006. Lysosomes as the target of yessotoxin in invertebrate and
707 vertebrate cell lines. Toxicology Letters 167, 75-83.

708 Martinez-Maqueda, D., Miralles, B., Recio, I., 2015. HT29 Cell Line. in: Verhoeckx, K., Cotter, P.,
709 Lopez-Exposito, I., Kleiveland, C., Lea, T., Mackie, A., Requena, T., Swiatecka, D., Wichers, H. (Eds.). The
710 Impact of Food Bioactives on Health: in vitro and ex vivo models, Cham (CH), pp. 113-124.

711 Natoli, M., Leoni, B.D., D'Agnano, I., Zucco, F., Felsani, A., 2012. Good Caco-2 cell culture practices. Toxicol In
712 Vitro 26, 1243-1246.

713 Ogino, H., Kumagai, M., Yasumoto, T., 1997. Toxicologic evaluation of yessotoxin. Nat. Toxins. 5, 255-259.

714 Okada, T., Narai, A., Matsunaga, S., Fusetani, N., Shimizu, M., 2000. Assessment of the Marine Toxins by
715 Monitoring the Integrity of Human Intestinal Caco-2 Cell Monolayers. Toxicology in vitro 14, 219-226.

716 Pan, F., Han, L., Zhang, Y., Yu, Y., Liu, J., 2015. Optimization of Caco-2 and HT29 co-culture in vitro cell models
717 for permeability studies. Int J Food Sci Nutr 66, 680-685.

718 Ray, R.M., Bhattacharya, S., Johnson, L.R., 2005. Protein phosphatase 2A regulates apoptosis in intestinal
719 epithelial cells. J Biol Chem 280, 31091-31100.

720 Reale, O., Huguet, A., Fessard, V., 2019. Novel Insights on the Toxicity of Phycotoxins on the Gut through the
721 Targeting of Enteric Glial Cells. Mar Drugs 17.

722 Reguera, B., Riobo, P., Rodriguez, F., Diaz, P.A., Pizarro, G., Paz, B., Franco, J.M., Blanco, J., 2014. Dinophysis
723 toxins: causative organisms, distribution and fate in shellfish. Mar Drugs 12, 394-461.

724 Ronzitti, G., Callegari, F., Malaguti, C., Rossini, G.P., 2004. Selective disruption of the E-cadherin-catenin system
725 by an algal toxin. Br J Cancer 90, 1100-1107.

726 Ronzitti, G., Hess, P., Rehmann, N., Rossini, G.P., 2007. Azaspiracid-1 alters the E-cadherin pool in epithelial
727 cells. Toxicol Sci 95, 427-435.

728 Ryan, G.E., Hess, P., Ryan, M.P., 2004. Development of a functional in vitro bioassay for azaspiracids (AZA)
729 using human colonic epithelial cells. Proceedings of the 5th International Conference on Molluscan Shellfish
730 Safety, Galway, Ireland, June 14-18, The Marine Institute.

731 Sedgwick, J.B., Menon, I., Gern, J.E., Busse, W.W., 2002. Effects of inflammatory cytokines on thepermeability of
732 human lung microvascular endothelial cell monolayers and differential eosinophil transmigration. Jounal
733 Allergy Clin Immunol 110, 752-756.

734 Serandour, A.L., Ledreux, A., Morin, B., Derick, S., Augier, E., Lanceleur, R., Hamlaoui, S., Moukha, S., Furger,
735 C., Bire, R., Krys, S., Fessard, V., Troussellier, M., Bernard, C., 2012. Collaborative study for the detection of toxic
736 compounds in shellfish extracts using cell-based assays. Part I: screening strategy and pre-validation study with
737 lipophilic marine toxins. Anal Bioanal Chem 403, 1983-1993.

738 Sosa, S., Ardizzone, M., Beltramo, D., Vita, F., Dell'Ovo, V., Barreras, A., Yasumoto, T., Tubaro, A., 2013.
739 Repeated oral co-exposure to yessotoxin and okadaic acid: a short term toxicity study in mice. Toxicon 76,
740 94-102.

741 Takenaka, T., Harada, N., Kuze, J., Chiba, M., Iwao, T., Matsunaga, T., 2014. Human Small Intestinal Epithelial
742 Cells Differentiated from Adult Intestinal Stem Cells as a Novel System for Predicting Oral Drug Absorption in
743 Humans. Drug Metabolism and Disposition 42, 1947-1954.

744 Tarantini, A., Lanceleur, R., Mourot, A., Lavault, M.T., Casterou, G., Jarry, G., Hogeveen, K., Fessard, V., 2015.
745 Toxicity, genotoxicity and proinflammatory effects of amorphous nanosilica in the human intestinal Caco-2 cell
746 line. Toxicol In Vitro 29, 398-407.

747 Terao, K., Ito, E., Managi, T., Yasumoto, T., 1986. Histopathological studies on experimental marine toxin
748 poisoning. I. Ultrastructural changes in the small intestine and liver of suckling mice induced by
749 dinophysistoxin-1 and pectenotoxin-1. Toxicon 24, 1141-1151.

750 Tor, L., 2015. Caco-2 Cell Line. The Impact of Food Bioactives on Health, pp. 103-111.

751 Tripuraneni, J., Koutsouris, A., Pestic, L., Hecht, G., 1997. The Toxin of Diarrheic Shellfish Poisoning, Okadaic
752 Acid, Increases Intestinal Epithelial Paracellular Permeability. Gastroenterology 112, 100-108.

753 Twiner, M.J., Hanagriff, J.C., Butler, S., Madhkoor, A.K., Doucette, G.J., 2012. Induction of apoptosis pathways
754 in several cell lines following exposure to the marine algal toxin azaspiracid. Chem Res Toxicol 25, 1493-1501.

755 Twiner, M.J., Rehmann, N., Hess, P., Doucette, G.J., 2008. Azaspiracid shellfish poisoning: a review on the
756 chemistry, ecology, and toxicology with an emphasis on human health impacts. Mar Drugs 6, 39-72.

757 Valdiglesias, V., Prego-Faraldo, M.V., Pasaro, E., Mendez, J., Laffon, B., 2013. Okadaic acid: more than a
758 diarrheic toxin. Mar Drugs 11, 4328-4349.

759 Vilarino, N., Louzao, C., Abal, P., Cagide, E., Carrera, C., Vieytes, M.R., Botana, L.M., 2018. Human Poisoning
760 from Marine Toxins: Unknowns for Optimal Consumer Protection. Toxins 10, 324.

761 Vilarino, N., Nicolaou, K.C., Frederick, M.O., Cagide, E., Alfonso, C., Alonso, E., Vieytes, M.R., Botana, L.M.,
762 2008. Azaspiracid substituent at C1 is relevant to in vitro toxicity. Chem Res Toxicol 21, 1823-1831.

763 Zhang, W., Xu, Y., Chen, Z., Xu, Z., Xu, H., 2011. Knockdown of aquaporin 3 is involved in intestinal barrier
764 integrity impairment. FEBS Lett 585, 3113-3119.

765